Terr. Atmos. Ocean. Sci., Vol. 26, No. 5, 493-502, October 2015 doi: 10.3319/TAO.2015.04.08.01(T)

One-Dimensional Velocity Structure of the Crust in Fujian, Southeast China

Hui-Teng Cai *, Xin Jin, and Shan-Xiong Wang

Earthquake Administration of Fujian Province, Fuzhou, China

Received 18 August 2014, revised 7 April 2015, accepted 8 April 2015

ABSTRACT

12095 P-wave phase data were selected in this study from four NW-oriented and four NE-oriented explosion sounding survey lines conducted along the coast and midland of Southeast China during the years 2010 and 2012. The 1-D crust P-wave velocity model was obtained in the continental margin of Southeast China (Fujian Province) using the travel time residual as the threshold and performing linear iterative inversion. This crust model includes 5 layers with the velocities being 5.04, 5.44, 6.06, 6.16, 6.39 km s^{-1}, respectively, with the bottom depths being 0.23, 2.82, 6.44, 18.81, 30.42 km, respectively, and the uppermost mantle velocity being 8.08 km s^{-1}. Compared with previous work the four P-wave phase data could effectively reflect the shallow and deep crust characteristics. The joint inversion method involves both the velocity and depth. The results in this paper could therefore be more reasonable and applicable than previous findings, with fairly good control in both the shallow and deep crusts. These findings have practical significance for compiling the earthquake travel time table and precisely locating earthquakes in this area. This work also provides an accurate preliminary model for subsequent 2-D and 3-D velocity structure inversions in the Southeast China (Fujian Province) continental margin.

Key words: Continental margin of Southeast China, 1-D crust velocity structure, Explosion, Linear inversion, Travel time residual

Citation: Cai, H. T., X. Jin, and S. X. Wang, 2015: One-dimensional velocity structure of the crust in Fujian, Southeast China. Terr. Atmos. Ocean. Sci., 26, 493-502, doi: 10.3319/TAO.2015.04.08.01(T)

1. INTRODUCTION

Seismic wave use as carriers to detect the Earth's internal structure has been the most effective method with the highest resolution thus far (Zhou and Xu 2010). With the development of global digital seismic observation technology and the construction of numerous observation networks along with continual advances in computer technology, earthquakes can now be located rapidly and their 3-D velocity structure inversion obtained. However, the precise location of earthquakes and the detailed detection of their 2-D and 3-D velocity structures require a 1-D velocity structure model that is simple, laterally homogenous and approximates the "true Earth" as closely as possible (Chiarabba and Frepoli 1997; Yang et al. 2004).

The typical early 1-D velocity structure research methods mainly include Herglotz-Wiechert, Gutenberg Inversion and τ(p) (Geiger 1912). However, the 1-D velocity structures of nearly all of these methods were attained using numerous earthquake travel time data. Due to uncertainty limitations these early methods are now rarely applied (Shearer 1999). At present the linear method is mainly applied to earthquake travel time to inverse the regional scale 1-D velocity structure, the most typical of which is the linear method along with the compiled module VELEST (Kissling 1988; Kissling et al. 1994) of the software SEISAN, which is widely used for model optimization (Havskov and Ottemöller 2001). This method and module was used in previous studies to improve the 1-D velocity model and enhance the earthquake location precision in Costa Rica, South Africa, Albania, and Sicily in Italy (Quintero and Kissling 2001; Musumeci et al. 2003; Ormeni 2009; Midzi et al. 2010). Mohamed and Miyashita (2001) inversed the 1-D P-wave velocity crust model in the northern Red Sea using this module. This method has been applied to many domestic areas like Beijing, Tianjin, Tangshan (Yu et al. 2003), the Three Gorges front area (Zhao et al. 2007), and Shandong (Li et al. 2012) and so on. Since the earthquake source parameter is unknown, source and velocity coupling problem exists in models that are jointly inversed based on the earthquake. As the explosion source parameter is given

* *Corresponding author*
E-mail: caihuiteng@126.com

compared with the earthquake, the 1-D velocity structure inversion precision for the explosion would be higher than that for the earthquake if the artificial seismic ray can be evenly distributed within the region.

The earliest 1-D crust velocity structure model available to the Southeast China (Fujian Province) continental margin is the "Local Earthquake Travel Time Table for South China" published in 1988 (Fan et al. 1990). The two-layer crust model was attained according to the earthquake observation data and part of the explosions from six provinces in South China. Later, Liao et al. (1988) presented the three-layer crust model applicable to the Shantou-Quanzhou and Quanzhou-Changle areas based on the deep seismic sounding profiles in Shantou-Quanzhou-Changle. Grounded on analyzing and comparing the previous results, Chen et al. (2005) provided a comprehensive 1-D average crust velocity structure model for Fujian Province after properly amending the three-layer crust model in Shantou-Quanzhou to further carry out the seismic tomography in this area. The above 1-D crust velocity structure model for Fujian Province was attained based on analog recordings in the 1980s and using forward modeling.

To address the above problems study data were selected from the four NW-oriented and four NE-oriented explosion sounding survey lines conducted along the Southeast China coast and midland during 2010 and 2012. The 1-D crust velocity structure in the Southeast China (Fujian Province) continental margin was studied using the travel time residual as the threshold to perform linear iterative inversion and compile the corresponding program.

2. GEOLOGICAL SETTINGS OF FUJIAN

The Southeast China (Fujian Province) continental margin has developed into a fault basin that features fault bays and plains in coastal areas. Daiyun Mountain is roughly the boundary between the distinct eastern and western sides. The fault and fault depression basins of Late Cretaceous-Paleogene periods lie mainly on the western side, with most of these basins at an extinction stage in the Quaternary period. The fault basin and bay developed well on the western side in the Quaternary period, with the longest axis NW oriented and often controlled by NW-oriented active faults. These faults have declined sharply since the Late Pleistocene period. For instance, the biggest river, lake, and sea stratum thickness in Fuzhou Basin and Longhai Plain at this stage is 63.78 and 81.03 m, respectively.

The fault structure is well developed and often exhibits large scale, long extension, cutting crust, and multistage activity characteristics. There are three NNE-NE-oriented large scale faults: Changle-Zhao'an Fault Zone (from the Min River Estuary to Nan'ao Island of Guangdong in its north and south respectively), Zhenghe-Dapu Fault Zone, and Shaowu-Heyuan Fault Zone. The main NNW-NW-oriented fault zones include the lower reaches of the Min River, Shaxian-Nanri Island, Yong'an-Jinjiang, Jiulong River, and Shanghang-Zhao'an (Fig. 1). These two sets of faults constitute the basic tectonic framework of the Southeast China continental margin.

There are moderate earthquakes across the coastal land in the research area, mainly within the Zhangzhou and Quanzhou basins, whereas the seismic activity weakens inland with a few scattered approximately M 5.0 earthquakes.

3. ARTIFICIAL SEISMIC SOUNDING PROJECTS

Artificial seismic sounding projects targeted for the continental margin of Southeast China (Fujian Province) were conducted from 2010 - 2012 by the Earthquake Administration of Fujian Province in coordination with the Geophysical Exploration Center of China Earthquake Administration. In these projects, "four longitudinal four horizontal" lines were deployed: four NW-oriented main detection survey lines, FJ1, FJ2, FJ3, and FJ4, and four NE-oriented auxiliary detection survey lines, FJ5, FJ6, FJ7, and FJ8 (Fig. 2), all of which composed the overall layout of the regional grid array. An independent observation system was still retained in the case of each survey line (which can be separated into 2-D profiles). The detection range could evenly cover most areas in the Southeast China (Fujian Province) continental margin. Eighteen explosion excitations were conducted and most of the shot locations (Fig. 2) were at the intersections of survey lines. The instruments used for collecting the explosion detection data were a seismic sounding special digital seismograph (Type PDS-2) and matched three-component seismic geophone (Type CDJ-6B). The project explosion observation data were treated and studied by performing comparisons and analyses (take the SP21 point excitation and the SP31 point excitation for example, Fig. 3 is the profile of the FJ2 longitudinal survey line, while Fig. 4 shows the profile of the FJ3 longitudinal survey line). Four phases, Pg, Pc, Pm, and Pn, were identified based on these studies (Table 1).

4. METHOD

According to Ray Theory (Shearer 1999), travel time t_i along the ray path L_i should be:

$$t_i = \int_{L_i} \frac{ds}{v(r)} \qquad i = 1, 2, ...m \tag{1}$$

In Eq. (1), r represents the position vector; $v(r)$ represents the wave velocity of r; m represents the total phase travel time data obtained from the explosion experiments. Equation (1) shows that travel time is a nonlinear function of the velocity and the interface depth (the source parameter is given in explosion). This equation can be converted into Eq. (2), in which x represents the influence parameter of velocity and

interface on the ray wave travel time and n is the number of influence parameters. Equation (3) was obtained based on using the Taylor first-order series on Eq. (2).

$$t_i = t_i[x(x_1, x_2, \ldots, x_j, \ldots, x_n)] \qquad j = 1, 2, \ldots n \tag{2}$$

$$t_i^{observation} = t_i^{preliminary\ model} + \sum_{j=1}^{n} \frac{\partial t_i}{\partial x_j} \Delta x_j \tag{3}$$

$$\frac{\partial t_i}{\partial x_j} = \frac{\left\{ \begin{matrix} t_i[x(x_1, x_2, \ldots, x_j + \partial x_j, \ldots, x_n)] \\ - t_i[x(x_1, x_2, \ldots, x_j, \ldots, x_n)] \end{matrix} \right\}}{\partial x_j} \tag{4}$$

$$\Delta t_i = t_i^{observation} - t_i^{preliminary\ model} = \sum_{j=1}^{n} \frac{\partial t_i}{\partial x_j} \Delta x_j \tag{5}$$

In the above equations, $t_i^{observation}$ is the travel time observed in the experiments; $t_i^{preliminary\ model}$ is the theoretical travel time corresponding to ray $t_i^{observation}$ in the preliminary model; $\frac{\partial t_i}{\partial x_j}$ in Eq. (4) signifies the linearization partial derivative operator. Typically when Eq. (3) is expressed as Eq. (5), Δt represents the travel time residual.

When Eq. (5) is converted into the compact form Eq. (6), the coefficient of Matrix Jacobi A would become Eq. (7). Generally there are the least square method, generalized inverse matrix method and damping least square method for Eq. (6) solutions.

$$\delta t = A \delta x \tag{6}$$

$$a_{ij} = \frac{\partial t_i}{\partial x_j} \begin{pmatrix} i = 1, 2, \ldots, m \\ j = 1, 2, \ldots, n \end{pmatrix} \tag{7}$$

5. CALCULATION PROCESSES

There are 5 steps for the calculation process as presented in Fig. 5.

Step 1. Build a preliminary inversion model. That is, the stratification method (Shearer 1999) is used in Phase Pg travel time data to build the crystal substratum velocity structure. The T2-X2 method (Zhang et al. 1994; Cerveny 2005) is used in Phase Pi travel time data to build the crystal reflector velocity structure. Linear fitting is used in Phase Pn travel time data to attain the uppermost mantle velocity. The preliminary inversion model could be built combining the above calculation results.

Step 2. Calculate the corresponding theoretical travel time, travel time residual and root mean square of travel time residual according to the preliminary model and observation epicenter distance.

Step 3. Calculate the linearization partial derivative operator according to the values in Eq. (4) to obtain the Matrix Jacobi A that can be combined with the travel time residual vector to build the inversion equation.

Step 4. Solve Eq. (6) using the generalized inverse matrix method to further revise the preliminary model.

Step 5. Judge whether the convergence condition is satisfied according to the root mean square of the travel time residual for the preliminary and revised models. If the condition is satisfied, the preliminary model would be replaced with the revised model to conduct the next iterative calculation. If the condition is not satisfied, this iterative preliminary model would be adopted as the last inversion model.

Using such methods and processes the author compiled the LIAE1D program to calculate the 1-D crust velocity structure in the Southeast China (Fujian Province) continental margin.

6. NUMERICAL SIMULATION

A numerical simulation experiment was designed for validating the methods and program mentioned in the preceding section. As shown in Fig. 6 the test model was sorted into four layers corresponding to the crystal substratum, the upper crust, the lower crust, and the uppermost mantle in the crust. The velocity and thickness of the upper three layers were 5.6, 6.2, 6.4, 8.1 km s^{-1}, and 3, 15, 12 km respectively. In the observation system the seismic source was located on Pile No. 0 km, whereas the receivers were located on Pile Nos. between 20 - 250 km with the interval 2 km. A total of 417 travel time data were received from the four sets of phases: Pg, Pc, Pm, and Pn (only the receiver exceeding the critical distance was used to observe the travel time in Pg and Pn). The layer velocity and layer thickness disturbance values were ±8% in the preliminary model corresponding the test model. The program LIAE1D was used to calculate the corresponding inversion model shown in Fig. 6. The travel time residual distributions are shown in Fig. 7. The results in Fig. 7 show that the upper and lower crust layer velocity and layer thickness, and the uppermost mantle velocity all coincide with the test model values. However, some errors are present in the crustal substratum velocity and thickness. This indicates that the results obtained were unreliable only when the refraction wave travel time was used to conduct the crystal substratum inversion. In practical applications the direct wave observed from the receivers must be used before the critical distance, i.e., the stratification method should be used to control the preliminary model in order to subdivide the crystal substratum.

7. DETERMINATIONS OF THE 1-D CRUSTAL VELOCITY STRUCTURES

We used the LIAE1D program to inverse the overall

1-D crust velocity structure and 1-D crust velocity structure models for the 8 longitudinal survey lines in the Southeast China continental margin (Tables 2 and 3). The theoretical travel time and the travel time observed in the tests are compared in Fig. 8. The root mean square values of the travel time residuals are listed in Table 4. The results in Fig. 8 and Table 4 show that the theoretical travel time calculated using the inversion results closely reflects the average variation trend in the test observational travel time. The travel time residual root mean square is between 0.0758 - 0.1312 s. This indicates that the inversed model approximates the "average model."

8. COMPARISONS BETWEEN PREVIOUS WORKS AND THIS STUDY

The earliest crust P-wave velocity structure models available for the Southeast China (Fujian Province) continental margin include the South China model and the Chen et al. (2005) results. Li et al. (2011) inversed the body wave velocity structure of the medium upper crust in Fujian Province based on the noise records obtained from the 25 Fujian Earthquake Network broadband stations. These three crust velocity structure models are shown in Table 5. The theoretical and observational travel time obtained for the three

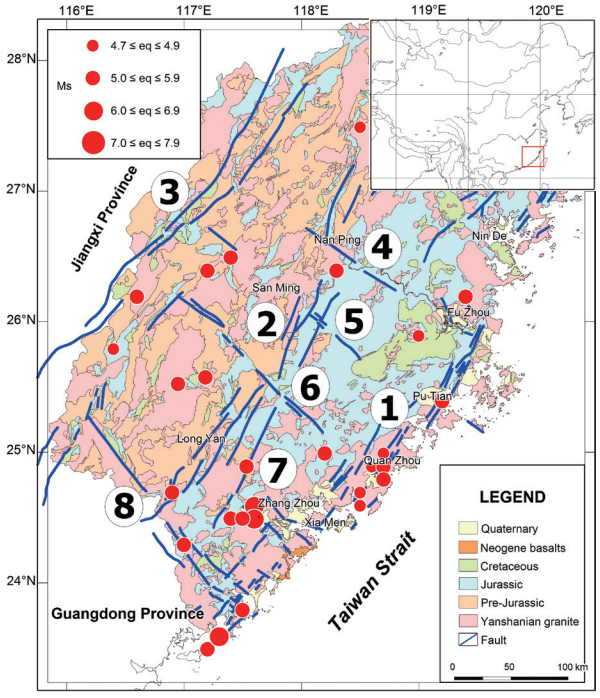

Fig. 1. Seismotectonic map in continental margin of Southeast China. NE-oriented fault: ① Changle-Zhao'an, ② Zhenghe-Haifeng, ③ Shaowu-Heyuan; NW-oriented fault: ④ Min River, ⑤ Shaxian-Nanri Island, ⑥ Yong'an-Jinjiang, ⑦ Jiulong River, ⑧ Shanghang-Yunxiao.

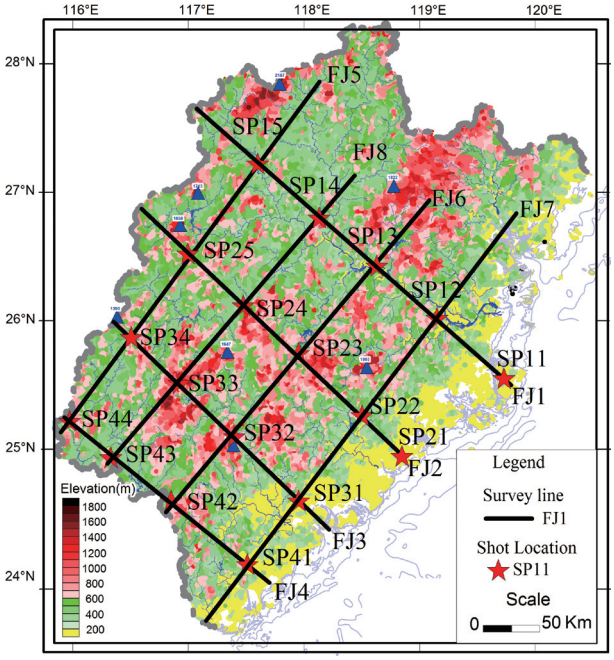

Fig. 2. Location map of survey lines and shots locations for the artificial seismic sounding project in continental margin of Southeast China (Fujian Province).

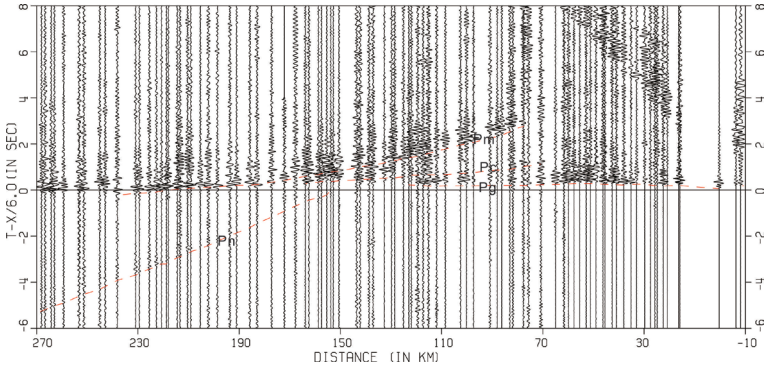

Fig. 3. Receiving records of FJ2 survey line from SP21 point excitation.

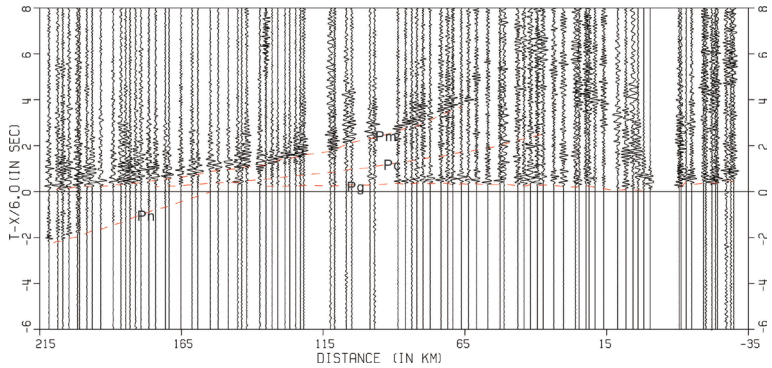

Fig. 4. Receiving records of FJ3 survey line from SP31 point excitation.

Table 1. Phase records and parameters used in inversion crust models (unit: number).

Phase	FJ1	FJ2	FJ3	FJ4	FJ5	FJ6	FJ7	FJ8	Continental Margin of Southeast China
Pg	235	361	289	278	227	154	192	150	3161
Pc	221	157	119	135	150	92	112	89	2259
Pm	206	198	153	169	197	122	141	115	4642
Pn	62	60	31	26	78	33	43	37	2033
Total	724	776	592	608	652	401	488	391	12095

Note: Phase Pg-wave means basement refraction wave; Phase Pc-wave means reflection wave for bottom boundary of upper crust (the interface of upper and lower crust); Phase Pm-wave means reflection wave of Moho profile; Phase Pn-wave means refraction wave for the uppermost mantle, where the Southeast China (Fujian Province) continental margin includes non-longitudinal phases.

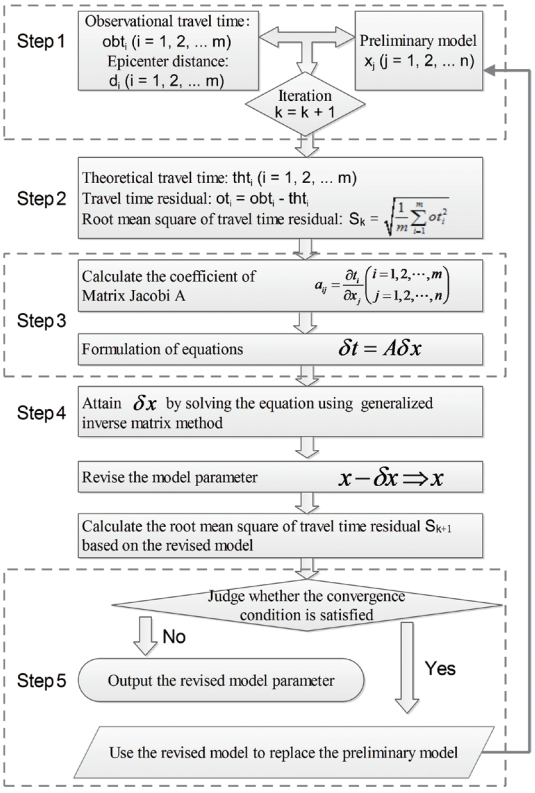

Fig. 5. Linear iteration inversion process.

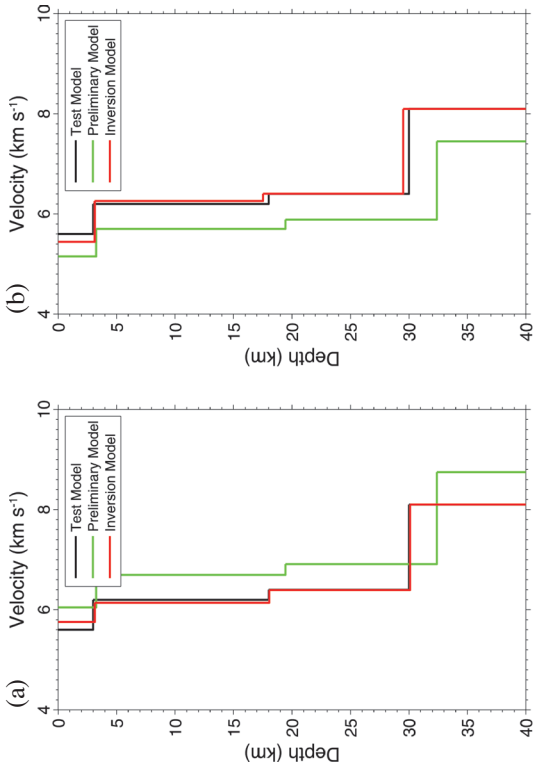

Fig. 6. Test, preliminary, and inversion model, (a) velocity +8%, interface +8%; (b) velocity -8%, interface +8%; (c) velocity +8%, interface -8%; (d) velocity -8%, interface -8%.

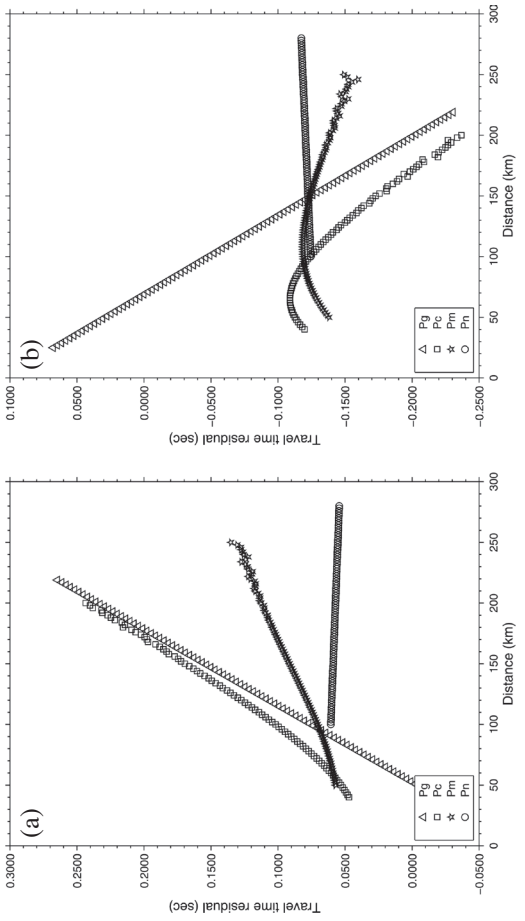

Fig. 7. Distributions of travel time residual, (a) velocity +8%, interface +8%; (b) velocity -8%, interface +8%; (c) velocity +8%, interface -8%; (d) velocity -8%, interface -8%.

Table 2. 1-D crust layer thickness in Southeast China (Fujian Province) continental margin (unit: km).

Position	FJ1	FJ2	FJ3	FJ4	FJ5	FJ6	FJ7	FJ8	Continental Margin of Southeast China
Crystal Substratum	0.70	0.69	0.62	0.01	0.52	0.72	0.34	0.74	0.23
	1.93	2.42	1.92	1.88	1.67	2.36	2.15	2.13	2.59
Upper Crust	3.82	3.54	4.58	4.38	4.12	3.89	4.21	3.96	3.62
	10.50	10.68	11.88	12.43	11.58	10.80	12.10	11.14	12.37
Lower Crust	13.97	14.34	13.36	12.85	13.22	13.95	12.54	13.43	11.61
Crust Thickness	30.92	31.67	31.73	31.55	31.11	31.72	31.34	31.40	30.42

Table 3. 1-D crust layer velocity in continental margin of Southeast China (Fujian Province) (unit: km s^{-1}).

Position	FJ1	FJ2	FJ3	FJ4	FJ5	FJ6	FJ7	FJ8	Continental Margin of Southeast China
Crystal Substratum	5.38	5.05	4.79	5.15	4.85	5.18	5.16	5.51	5.04
	5.77	5.88	5.61	5.38	5.63	5.44	5.58	5.84	5.44
Upper Crust	5.99	5.98	5.98	5.99	5.94	5.98	6.01	5.95	6.06
	6.15	6.14	6.21	6.16	6.13	6.16	6.21	6.13	6.16
Lower Crust	6.53	6.43	6.54	6.58	6.37	6.48	6.61	6.43	6.39
Top of Upper Mantle	8.10	8.13	8.03	8.09	8.08	8.12	8.09	8.07	8.08

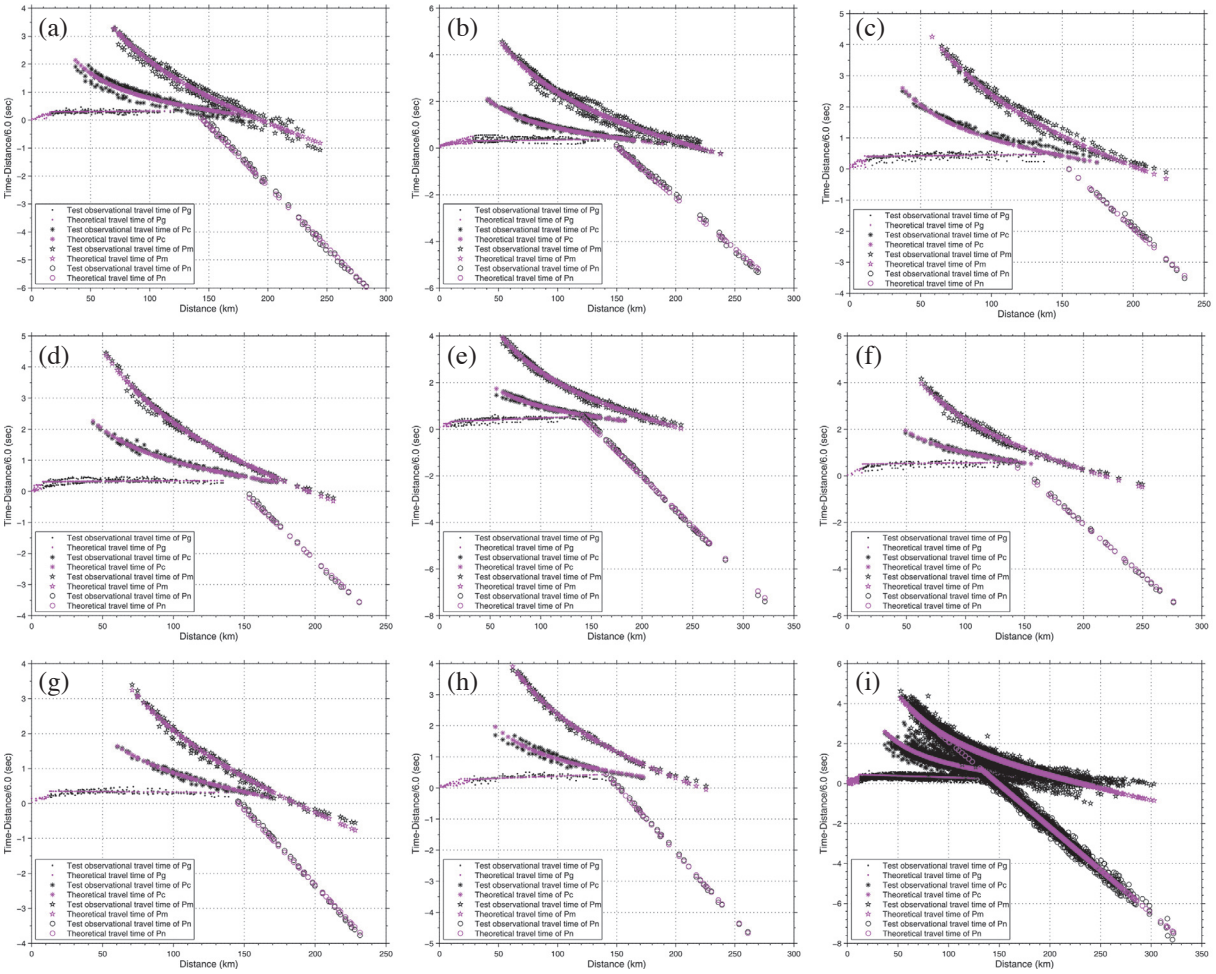

Fig. 8. Comparisons of theoretical travel time, observational travel time before and after the inversion. (a) FJ1 survey line; (b) FJ2 survey line; (c) FJ3 survey line; (d) FJ4 survey line; (e) FJ5 survey line; (f) FJ6 survey line; (g) FJ7 survey line; (h) FJ8 survey line; (i) Southeast China (Fujian Province) continental margin.

Table 4. Root mean squares of travel time residuals (unit: s).

FJ1	FJ2	FJ3	FJ4	FJ5	FJ6	FJ7	FJ8	Continental Margin of Southeast China
0.1312	0.1273	0.1040	0.0757	0.0913	0.1098	0.0781	0.0758	0.2223

Table 5. Four kinds of 1-D crust velocity structure models in Southeast China (Fujian Province) continental margin.

Position	Current Results		Model of South China		Results of Chen Xiangxiong		Results of Li Jun	
	Thickness (km)	Velocity (km s^{-1})	Thickness (km)	Velocity (km s^{-1})	Thickness (km)	Velocity (km s^{-1})	Thickness (km)	Velocity (km s^{-1})
Crystal Substratum	0.23 2.59	5.04 5.44	-	-	3	5.57	3	5.54
Upper Crust	3.62 12.37	6.06 6.16	21.4	6.01	14.25	6.2	19.0	6.02
Lower Crust	11.61	6.39	11	6.88	12.25	6.81	10.4	6.61
Top of Upper Mantle	-	8.08	-	7.98	-	8.1	-	7.98

models are compared in Fig. 9. The travel time residual root mean squares feature distinct phases as shown in Fig. 10.

Collectively, the models and results in Table 5 and Figs. 9 and 10 reveal that:

(1) As the crystal substratum was not included in the South China model, the Pg phase was compared using only the results selected from this study and the studies of Chen et al. (2005) and Li et al. (2011). As shown in Table 5, when the upper crust velocity of 6.2 km s^{-1} was selected from the Chen et al. (2005) results, the deviations in the theoretical travel time and tested observational travel time were large. Moreover, although the overall upper crust velocity and crystal substratum parameters are similar in the Li et al. (2011) results and this study, the travel time residual root mean squares obtained for the phase Pg are also similar Compared with the Li et al. (2011) results, the results of this study more accurately represent the average trend for the tested observational travel time shown in Fig. 9a.

(2) Comparing the Pc and Pm phases shows that in the three previous models the test observational travel time deviations are larger than those in the current model. This is largely because only a few travel time samples from phase Pc were used for calculating the South China model. In the Chen et al. (2005) study the Fujian Province 1-D model was presented based mainly on the Changle-Quanzhou-Shantou sounding profile. The limitation here is that the line was used to replace the surface. Li et al. (2011) reported that the surface wave frequency scattering curve precision was high over a short period but the surface wave frequency scattering curve deviation was large over a long period (i.e., the inversion precision was high in the case of shallow results). The medium lower crust was presented combined mainly with the South China model and consequently, certain deviations existed in the medium lower crust phase case in the model theoretical travel time and tested observational travel time in the results for both Chen et al. (2005) and Li et al. (2011).

(3) A comparison of the phase Pn shows that the results of this study approximate the model of South China, and both of these models reflect the average variation trend in the test observational travel time, with the root mean squares of the travel time residual being 0.217 and 0.313 s, respectively. This indicates that the phase Pn was controlled effectively in the two models.

9. CONCLUSION

This paper presented the results obtained from artificial sounding project travel time data conducted using a 3-D observation system in the Southeast China (Fujian Province) continental margin and the linear iterative inversion method. The proposed results are more accurate and applicable than those from the other three models developed for this area. The proposed results can be controlled effectively in both shallow and deep crusts. The proposed results are therefore of practical significance for compiling earthquake travel time tables and precisely locating earthquakes in this area. They also provide an accurate preliminary model for subsequent 2-D and 3-D velocity structure inversions in the Southeast China (Fujian Province) continental margin.

Acknowledgements I would like to extend my heartfelt gratitude to the working staff that made laborious efforts to collect field data from the Fujian Province and Geophysical Exploration Center of China Earthquake Administrations.

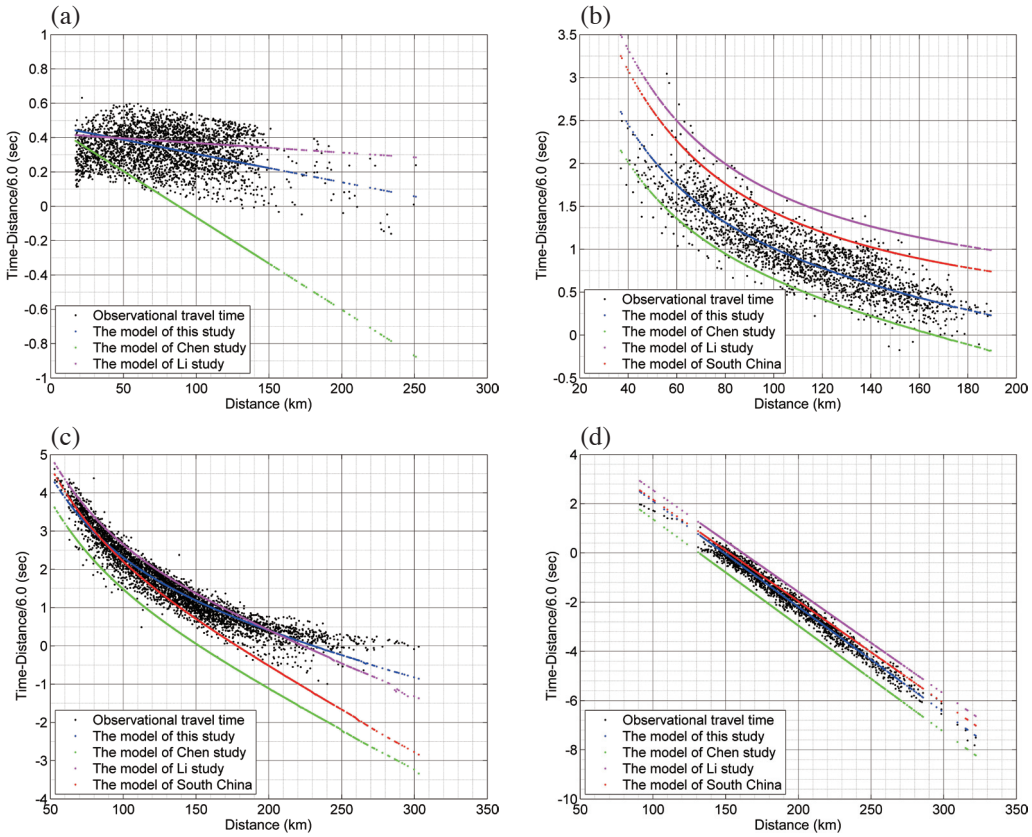

Fig. 9. Comparisons of theoretical travel time and test observational travel time for four models. (a) Wave Pg; (b) Wave Pc; (c) Wave Pm; (d) Wave Pn.

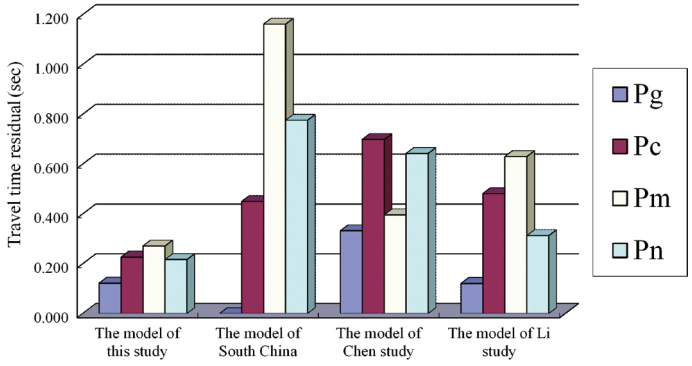

Fig. 10. Root mean squares of travel time residual with different phases for four models.

My sincere appreciation also goes to the attentive and valuable guidance from Researcher Wang Chunyong, Researcher Wang Fuyun, Researcher Zheng Sihua, and Director Zhang Long.

REFERENCES

Cerveny, V., 2005: Seismic Ray Theory, Cambridge University Press, Cambridge, 724 pp.

Chen, X., S. Lin, Z. Li, T. Bao, and Z. Zhou, 2005: Preliminary 1-D model of crust velocity structure in Fujian-Taiwan region. *Earthquake*, **25**, 61-68. (in Chinese)

Chiarabba, C. and A. Frepoli, 1997: Minimum 1D velocity models in Central and Southern Italy: A contribution to better constrain hypocentral determinations. *Ann. Geophys.*, **XL**, 937-954, doi: 10.4401/ag-3888. [Link]

Fan, Y., J. Lin, R. Hu, and Z. Luo, 1990: The development of travel timetable for near earthquake in South China. *South China Seismol. J.*, **10**, 1-16. (in Chinese)

Geiger, L., 1912: Probability method for the determination

of earthquake epicenters from the arrival time only. *Bull. St. Louis. Univ.*, **8**, 60-71.

Havskov, J. and L. Ottemöller, 2001: SeisAn: The Earthquake Analysis Software, University of Bergen, Norway.

Kissling, E., 1988: Geotomography with local earthquake data. *Rev. Geophys.*, **26**, 659-698, doi: 10.1029/RG026i004p00659. [Link]

Kissling, E., W. L. Ellsworth, D. Eberhart-Phillips, and U. Kradolfer, 1994: Initial reference models in local earthquake tomography. *J. Geophys. Res.*, **99**, 19635-19646, doi: 10.1029/93JB03138. [Link]

Li, B., X. Cui, Q. Ye, and C. Yu, 2012: Study of 1D velocity model in Shandong area. *North China Earthq. Sci.*, **30**, 1-6. (in Chinese)

Li, J., X. Jin, T. Bao, S. Lin, Y. Wei, and H. Zhang, 2011: The wave velocity structure of upper shell in Fujian estimated by the noise records. *Earthquake Res. China*, **27**, 226-234. (in Chinese)

Liao, Q. L., Z. M. Wang, and P. L. Wang, 1988: Explosion seismic study of the crustal structure in Fuzhou-Quzhou-Shantou region. *Chinese. J. Geophys.*, **31**, 270-280. (in Chinese)

Midzi, V., I. Saunders, M. B. C. Brandt, and T. Molea, 2010: 1-D velocity model for use by the SANSN in earthquake location. *Seismol. Res. Lett.*, **81**, 460-466, doi: 10.1785/gssrl.81.3.460. [Link]

Mohamed, H. and K. Miyashita, 2001: One-dimensional *P*-wave velocity structure in the northern Red Sea area, deduced from travel time data. *Earth Planets Space*, **53**, 695-702, doi: 10.1186/BF03352397. [Link]

Musumeci, C., G. Di Grazia, and S. Gresta, 2003: Minimum 1-D velocity model in Southeastern Sicily (Italy) from local earthquake data: An improvement in location accuracy. *J. Seismol.*, **7**, 469-478, doi: 10.1023/B:JOSE.0000005716.42446.da. [Link]

Ormeni, R., 2009: Crustal structures beneath the seismogenic zones and lateral velocity contrasts across deep faults of Albania. *J. Balkan Geophys. Soc.*, **12**, 1-8.

Quintero, R. and E. Kissling, 2001: An improved P-wave velocity reference model for Costa Rica. *Geofís. Int.*, **40**, 3-19.

Shearer, P. M., 1999: Introduction to Seismology, Cambridge University Press, Cambridge, 260 pp.

Yang, Z., X. Yu, Y. Zheng, Y. Chen, X. Ni, and W. Chan, 2004: Earthquake relocation and 3-dimensional crustal structure of P-wave velocity in central-western China. *Acta Seismol. Sin.*, **17**, 20-30, doi: 10.1007/BF03191391. [Link]

Yu, X., Y. Chen, and P. Wang, 2003: Three-dimensional P velocity structure in Beijing area. *Acta Seismol. Sin.*, **16**, 1-15. (in Chinese)

Zhang, C., J. Zhao, Q. Ren, X. Zhang, and Z. Zhu, 1994: Study on crust and upper mantle structure in North Henan and its surroundings. *Seismol. Geol.*, **16**, 243-253. (in Chinese)

Zhao, X., Q. Li, and J. Cai, 2007: On minimum 1D velocity model applied in three gorges reservoir area. *J. Geodesy Geodyn.*, **27**, 1-7. (in Chinese)

Zhou, S. and Z. Xu, 2010: Modern Seismology Tutorial, Beijing University Press, Beijing. (in Chinese)